

Efficacy of Borides in Grain Refining Al-Si Alloys



LEANDRO BOLZONI and NADENDLA HARI BABU

The grain refining efficacy of titanium, aluminum, and niobium borides, as well as niobium aluminides, introduced *via* commercial and lab made master alloys on Al-Si alloys was investigated. Significant grain refinement is achieved *via* the introduction of these heterogeneous nuclei regardless of their chemistry, stoichiometry of the master alloy, and addition rate. However, the grain refinement is affected by variable such as contact time, as the inoculating particle may sediment or be poisoned, and cooling rate. Specifically, a faster cooling rate generally leads to finer grains due to the lower time for grain growth. In the case of borides, the chemical inoculation efficiency is greatly affected by their thermodynamic stability in molten Al-Si alloys. Conversely, the grain refining potency of peritectic Al_3Nb remains unaffected. The underlying grain refining mechanism was finally investigated using current models based on the growth restriction factor Q to simultaneously consider the effect of nucleant potency and alloy chemistry. Among Ti-, Al-, and Nb-based borides with similar particle size and distribution, the latter are the most efficient to grain refine Al-Si alloys.

<https://doi.org/10.1007/s11661-018-5017-1>
© The Author(s) 2018

I. INTRODUCTION

THE control of nucleation is a fundamental aspect in many scientific disciplines such as chemical engineering, atmospheric science, plants biology, and food industry as well as engineering materials like superconductors and metals. The addition of heterogeneous substrates to control and enhance the nucleation stage is a common practice known as chemical inoculation. In the case of engineering alloys, inoculation of the molten metal leading to finer grains is highly beneficial as the fluidity of the alloy increases, and the number of defects and micro- and macro-porosity decreases.^[1] The facilitated casting process is also economically important because the quality of the casting is improved and the rejection rate reduced.^[2] Chemical inoculation of Al alloys is a standard procedure and is normally done by adding Al-Ti-B master alloys, also called grain refiners. The most widely used commercial Al-Ti-B master alloys, Al-5Ti-1B in Europe and Al-3Ti-1B in USA (if not stated differently, compositions are in wt pct), contain TiB_2 particles and have Ti/B weight ratio $> 2.2/1.0$ and, therefore, are defined as hyper-stoichiometric compositions. Excess Ti contributes to the refinement of the cast structure due to its high growth restriction factor in

Al.^[3] Because of more than 60 years of development and improvement, the addition of Al-Ti-B master alloys to wrought Al alloys, when the Si content is generally < 2 pct, is quite optimized.

The efficacy of commercial Al-Ti-B master alloys in refining the cast structure of Al and wrought Al alloys was promoted and is well known. For the sake of simplicity, this chemical inoculation procedure was adopted for Al-Si alloys assuming that the same benefits could be obtained in shape castings such as engine blocks, wheels, and pistons used in the transportation sector. Nonetheless, it has been shown that Al-Ti-B master alloys are far from being effective in refining the structure of Al-Si alloys.^[4] Research on the topic showed that Ti reacts with the Si of the Al-Si alloys forming Ti silicides, a phenomenon known as poisoning of the melt.^[5-8] Specifically, it was found that a layer of Ti_xSi_y is formed on top of the TiB_2 particles annihilating their ability to promote the nucleation of α -Al grains. This is due to the unfavorable lattice mismatch between Ti silicides and Al,^[8] a key factor to guarantee effective heterogeneous nucleation.

Research studies about alternative approaches investigated to effectively refine the cast structure of Al-Si alloys are available in the literature. Specifically, the effect of (i) higher addition rate of hyper-stoichiometric Al-Ti-B master alloys (*i.e.*, Al-5Ti-1B),^[5] (ii) stoichiometric (*i.e.*, Al-2.2Ti-1B) and sub-stoichiometric (*e.g.*, Al-3Ti-3B) compositions,^[5,9,10] (iii) Al-Ti-C master alloys,^[5,11,12] (iv) Al-Ti-B-C master alloys,^[13] and (v) Ti-free master alloys (*e.g.*, Al-3B)^[5,10,14] have lately been investigated. Nevertheless, as the problem is related to the reactivity of Ti, approaches (i-iv) are not intrinsically

LEANDRO BOLZONI is with the Waikato Centre for Advanced Materials (WaiCAM), The University of Waikato, Private Bag 3105, Hamilton 3240, New Zealand. Contact e-mail: leandro.bolzoni@gmail.com NADENDLA HARI BABU is with the BCAST, Brunel University London, Kingston Lane, Uxbridge UB8 3PH, UK.

Manuscript submitted July 31, 2018.

Article published online December 7, 2018

eliminating the problem. For the latter approach (v), it was found that the Al-3B master alloy performs very well if the Al-Si alloys are Ti-free^[15]; however, this is almost never the case for commercial Al-Si alloys where Ti is always present as impurity (~ 0.1 pct). When the Ti content is > 0.04 pct, Al-B master alloys have similar behavior to Al-Ti-B master alloys (*i.e.*, Al-5Ti-1B and Al-3Ti-3B)^[15] because AlB₂ is less stable than TiB₂ in the Al melt.^[16–18]

We recently reported that the cast structure of Al-Si alloys can efficiently be refined *via* inoculation by means of Nb + B addition and, as a consequence of the low yield of Nb and B recovery, we focused on the performance of a master alloy with Al-2Nb-2B nominal composition produced at lab scale.^[19,20] By means of a comparative study, in this work we address the following unresolved issues about the grain refinement of commercial Al-Si alloys: (i) effect of stoichiometry and addition rate of Al-Ti-B master alloys, (ii) effect of the addition and addition rate of Al-B master alloys, (iii) effect of addition of Al-Nb master alloy, (iv) effect of the use of different borides (*i.e.*, TiB₂, AlB₂, and NbB₂), and (v) effect of the processing conditions such as contact time and cooling rate. The aim of our work is to present and discuss the potentials and limitations of chemical inoculation considering the most critical variables affecting the performances and efficacy of the different method available to refine the cast structure of commercial Al-Si alloys on the basis of currently available models.

II. EXPERIMENTAL PROCEDURE

A. Materials

Our comparative study was done using a commercial Sr-modified A354 alloy (Al-9Si-1.8Cu-0.55Mg-0.15-Fe-0.12Ti) normally used to manufacture high-performance engine blocks *via* sand casting (*i.e.*, very slow cooling rate). Among hypoeutectic Al-Si alloys, the A354 was chosen as the higher the Si content the coarser the grain size^[2] and the more difficult is to refine the grain size. This gives a better idea about the intrinsic potency of the different heterogeneous nucleation substrates added. Commercial Al-5Ti-1B, Al-1.7Ti-1.7B and Al-5B master alloys were supplied by AMG, who also provided an in-house made Al-7Nb master alloy.

Our Al-2Nb-2B master alloy prepared at lab scale using the procedure previously reported^[19,20] was also studied for comparison. Sections of the master alloys were cut and prepared for metallographic analysis using the standard methodology: grinding plus polishing with OPS. Microstructural analysis was done either using a Carl Zeiss Axioskop-2 MAT optical microscope or a Zeiss SUPRA 35VP FEG-SEM. The latter was also employed for the analysis of deep-etched sections of the master alloys. TEM samples were manually ground to roughly 60 μm in thickness and further thinned using a ion polishing equipment (5 kV, incident angle of 6 deg), while the analysis was done on a JEOL 2200F-TEM operated at 200 keV. The details of the materials and variables considered in this study to quantify the “effect of heterogeneous nucleation substrates” are listed in Table I.

B. Inoculation Experiments

The reference A354 alloy already contains 0.12 pct Ti (Table I). Addition rates equivalent to 0.05 and 0.1 pct of the main chemical element of the master alloys were investigated (Table I). It is worth mentioning that the standard addition rate for commercial Al-Ti-B master alloys, independently of their stoichiometry, is generally 0.0001 pct Ti (*i.e.*, ~ 2 kg of Al-5Ti-1B per ton of melt). However, literature^[5] suggests to use higher addition rates for Al-Si alloys and, therefore, we investigated additions of Ti and B as high as 0.1 pct. The A354 alloy was melted and held at 760 °C for 1 hour prior to chemical inoculation; casting into a 30-mm cylindrical steel mould (preheated at 250 °C) was done at 740 ± 3 °C. The cooling rate achieved under these casting conditions is 2 °C/s as measured by means of K-Type thermocouples.^[19,20] Apart from the effect of the

Table II. Chemical Composition of the Alloys Used to Study the “Effect of Alloy Chemistry”

Alloy	Alloying Elements (Pct)						
	Si	Cu	Fe	Mg	Zn	Mn	Ti
A1	9.9	—	0.1	—	—	—	—
A2	7	0.054	0.154	0.35	0.054	0.067	0.12
A3	7	0.054	0.154	0.65	0.054	0.067	0.12
A4	9	1.8	0.154	0.55	0.1	0.75	0.12

Table I. Details of the Materials and Variables Considered in this Study to Quantify the “Effect of Heterogeneous Nucleation Substrates”

Material	Designation	Addition Rate	Fading	Effect of Cooling Rate
A354 (0.12 pct Ti)	Reference	—	✓	✓
Al-5Ti-1B	Al-5Ti-1B	0.1 pct Ti	✓	—
Al-1.7Ti-1.7B	Al-1.7Ti-1.7B	0.05 pct Ti	—	✓
		0.1 pct Ti	✓	✓
Al-5B	Al-5B	0.05 pct B	✓	✓
		0.1 pct B	✓	✓
Al-7Nb	Al-7Nb	0.1 pct Nb	✓	—
Al-2Nb-2B	Al-2Nb-2B	0.05 pct Nb	—	✓
		0.1 pct Nb	✓	✓

intrinsic chemistry of the inoculating phases, the effect of contact time was also evaluated (Table I). For that, fading experiments between 15 minutes and 7 hours were carried out. The A354 alloy was initially inoculated with the different master alloys and after an initial manual stirring, the alloy was left to repose until the completion of the targeted contact time. 30-mm cylindrical castings from 740 ± 3 °C were then obtained. Castings solidified using a cooling rate of 0.5 °C/s were also produced to study the effect of cooling rate (Table I). The same inoculation and casting conditions previously described were used for consistency. Samples were cast after 15 minutes of contact time for direct comparison.

C. Effect of Alloy Chemistry

The effect of the alloy chemistry on the grain refining capability using samples solidified at 0.5 °C/s, cast at 740 ± 3 °C without and with chemical inoculation with the previously mentioned master alloys, was studied. For that, Al-Si alloys with different amount of alloying elements were considered. The chemical composition of the alloys measured *via* optical emission spectroscopy is shown in Table II.

D. Characterization of the Castings

The microstructural study carried out on the 30-mm cylindrical castings was done on the cross section located at approximately 20 mm from the bottom of the samples and at roughly half of the diameter of the cylindrical section (see inset in Figure 1(a)). This is because in some materials, especially the reference A354 alloy, columnar grains were formed in the outer part of the castings upon solidification. For the same reason, the microstructural study on the castings solidified at 0.5 °C/s was done on the cross section located at 40 mm from the surface of the castings and one-third of the width of the section (see inset in Figure 1(b)). Classical

metallographic steps were taken to prepare the cross section of the castings for grain size measurements which were performed as per the intercept method (ASTM E112). For that, samples were submerged in a HBF₄ solution and anodized using a 10 V/1 A current. The opposite cross section of the castings was used for visual analysis, for which the samples were macroetched with the Tucker solution (15 ml HF + 15 ml HNO₃ + 45 ml HCl + 25 ml H₂O).

III. RESULTS

A. Reference A354 Al-Si Alloy

Data are available in the literature about the grain size of commercial Al-Si alloys without and with inoculation. However, variations in composition and impurity level as well as solidification conditions lead to changes in grain structure. For instance, we previously demonstrated that the superheating of Al-Si alloys has a strong effect on the size of their cast structure.^[21] Therefore, it is necessary to establish reference data (microstructure and grain size) in this work. Figure 1 presents the variation of the grain size with contact time and cooling rate of the reference A354 alloy. It is shown that independently of the time at temperature or cooling rate, the reference alloy has a coarse dendritic structure (micrographs as inset in Figure 1). The solidification of the A354 alloy begins by heterogeneous nucleation in the melt near the wall of the die followed by columnar growth (macrographs as inset in Figure 1). Solute enrichment at the solidification front and reduction of the thermal gradient leads to the formation of dendritic grains in the interior of the casting. The locations where grain size measurements were performed are also highlighted. These locations and the correlated grain size (~ 1500 μm) will be taken as reference. A lower cooling rate leads to a somewhat coarser microstructure.^[22] Moreover, it can be noticed the high variability

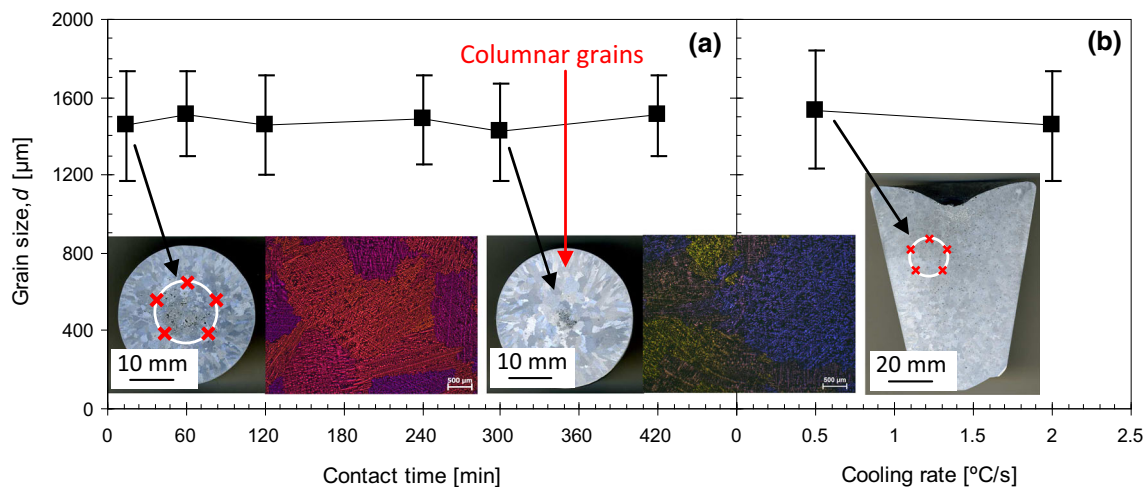


Fig. 1—Variation of the grain size (d) for the reference A354 alloy. (a) Effect of contact time and (b) effect of cooling rate. The cast structure of the reference is composed of dendritic α -Al grains and has columnar grains on the outer part of the castings (see macrographs as inset). The locations where the polarized light micrographs (examples as inset) for grain size measurements were taken are also labeled.

of the measurements which corresponds to highly heterogeneous non-equiaxed dendritic grains.

B. Inoculation with Ti-Based Master Alloys

Different studies in the literature report that hyper-stoichiometric (e.g., Reference 9) and sub-stoichiometric (e.g., Reference 5) Al-Ti-B master alloys can refine the cast structure of commercial Al-Si alloys. However, comparison with data available in the literature would be influenced by other processing variables such as composition of the alloys, inoculation procedure, and solidification conditions. Therefore, in this work inoculation of the A354 alloy with Al-5Ti-1B and Al-1.7Ti-1.7B was used so as to have a direct comparison of the potency of the different inoculants eliminating the effect of other variables. Figure 2 confirms that Al-Ti-B master alloys refine, to some extent, the cast structure of Al-Si alloys. Grain sizes in

the range of 200 μm are normally obtained when inoculating pure Al and wrought Al alloys with commercial Al-Ti-B master alloys. Nevertheless, from Figure 2 it can be seen that although of the 0.1 pct Ti addition, inoculation of the A354 alloy initially reduces the grain size down to only $\sim 800 \mu\text{m}$. The efficacy of the substrates is completely lost after 3 to 5 hours of contact time (Figure 2(a)) due to the sedimentation and poisoning of the TiB_2 particles. Cooling rate and addition level (Figure 2(b)) have a minor effect on the final cast structure. Inoculation of Al-Si alloys with Al-Ti-B master alloys does not permit to obtain a fully equiaxed structure as columnar grains are present in the castings, especially in the case of the sub-stoichiometric Al-1.7Ti-1.7B master alloy (see inset in Figure 2). This indicates that nucleation simultaneously happened heterogeneously from the melt near the wall of the die and from the TiB_2 substrates added.

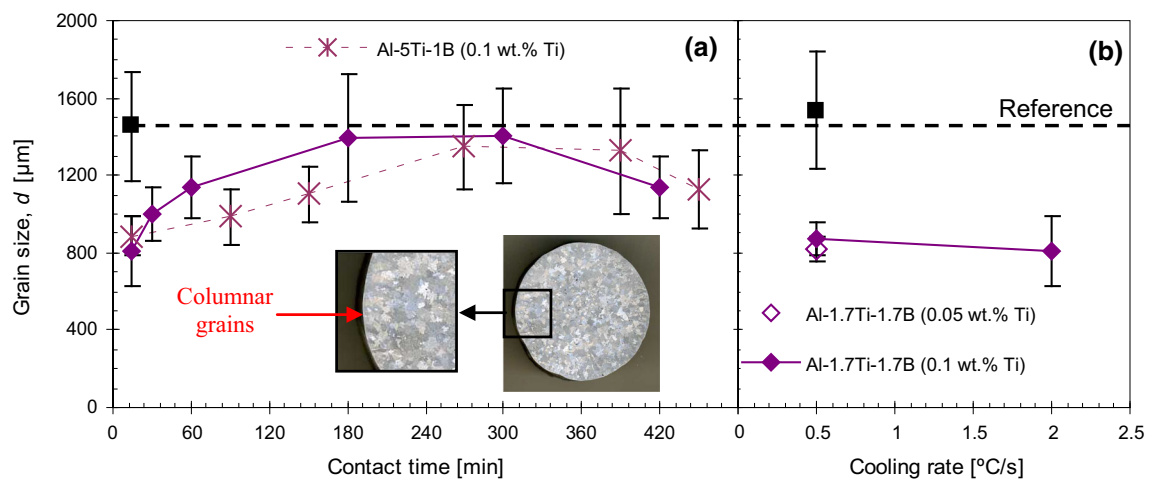


Fig. 2—Variation of the grain size (d) for the reference A354 alloy inoculated with Ti-based master alloys. (a) Effect of contact time and (b) effect of cooling rate. Inset: photo of the macroetched samples inoculated with 0.1 pctTi via Al-1.7Ti-1.7B master alloy.

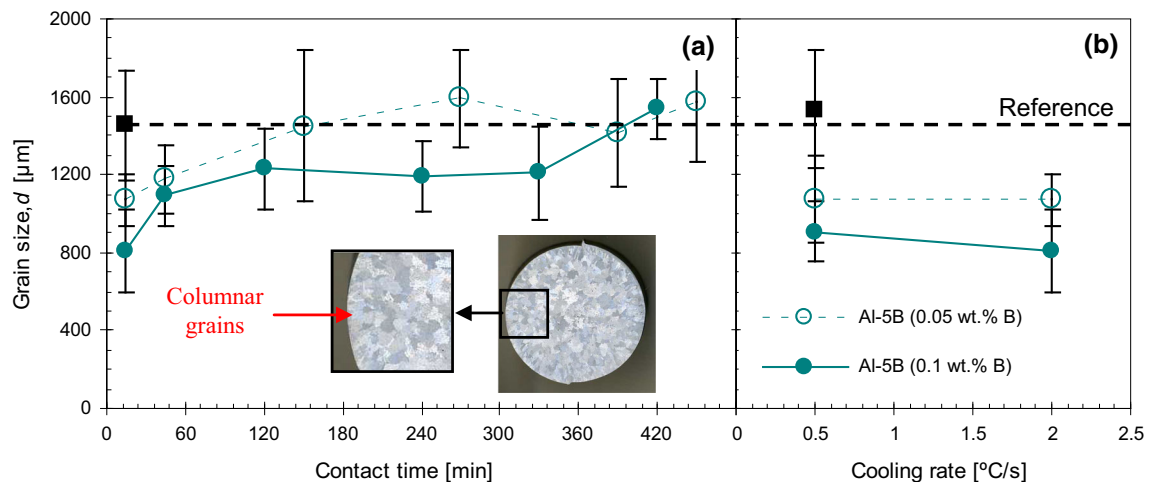


Fig. 3—Variation of the grain size (d) for the reference A354 alloy inoculated with B-based master alloy. (a) Effect of contact time and (b) effect of cooling rate. Inset: photo of the macroetched samples inoculated with 0.1 pctB via Al-5B master alloy.

C. Inoculation with B-Based Master Alloy

The addition of Ti-free master alloys has been previously studied and data are available in the literature (e.g., Reference 14). It is clear that Al-B master alloys are very effective in Ti-free Al-Si alloys, such as in binary and ternary Al-Si alloys prepared by high-purity materials (> 99.999 pct) as demonstrated by Chen *et al.*^[23] Nevertheless, when Ti is present as impurity, the performances of Al-B master alloys are comparable to those of commercial Al-Ti-B master alloys.^[15] This is because TiB₂ is much more stable than Al borides inside molten Al and thus Al borides transform into Ti borides.^[16–18] Experiments on the inoculation of the A354 alloy with the Al-5B master alloy confirm the initial promotion of heterogeneous nucleation. Such as in the case of Al-Ti-B master alloys, the potency of the heterogeneous substrates decreases with an increase of the contact time (Figure 3(a)) due to sedimentation and poisoning. The effect of cooling rate and addition level on the size of the grains constituting the cast structure is fairly evident. The lower the addition rate (*i.e.*, 0.05 vs 0.1 pct) and the lower the cooling rate (Figure 3(b)), the coarser the cast structure. As for the previous case where Ti-based substrates were used to promote heterogeneous nucleation, the addition of Al-B master alloys cannot completely suppress the formation of columnar grains during solidification of Al-Si alloys (see inset in Figure 3).

D. Inoculation with Nb-Based Master Alloys

In our previous study that led to the development of Nb + B inoculation, we analyzed the effect of the addition of Nb to pure Al but not to Al-Si alloys. We show in Figure 4 that the addition of the Al-7Nb master alloy can refine the cast structure of Al-Si alloys as much as commercial Al-Ti-B and Al-B master alloys because after 15 min the grain size is reduced to roughly 800 μm .

However, conversely to the commercial master alloys, the efficacy of the Al-7Nb master alloy is not affected by how long the heterogeneous nuclei stay in contact with the molten alloy as the grain size remains stable for as long as 7 hours. The grain refinement obtained by the addition of the Al-7Nb master alloy is due to the introduction of copious heterogeneous substrates as the addition rate of 0.1 pctNb is lower than the maximum solubility (*i.e.*, 0.15 pctNb^[24]). It is worth mentioning that the addition of the Al-7Nb master alloy to the A354 alloy almost completely prevents the formation of columnar grains growing in the melt from the grains nucleated near the wall of the die. A much narrower annular composed of columnar grains was present near the outer surface of the castings.

The lab made Al-2Nb-2B master alloy we developed contains Nb-based substrates (*i.e.*, Al₃Nb and NbB₂)^[25] which are isomorphous to the Ti-based substrates (*i.e.*, Al₃Ti and TiB₂) present in commercial Al-Ti-B master alloys. The combined addition of Nb and B permits to refine the cast structure of Al-Si alloys to a greater extent as after 15 min the grain size is < 300 μm (Figure 4(a)). The grain size slightly increases with the contact time and with the solidification time (Figure 4(b)). Yet, the grain size of the A354 alloy inoculated with the Al-2Nb-2B master alloy is much finer and the associated standard deviation is consequently much lower (*i.e.*, more homogeneous equiaxed grain structure). This study further shows that inoculation of Al-Si alloys with Nb-based substrates entirely suppresses the formation of columnar grains and thus the formation of the columnar-to-equiaxed transformation zone.^[25] The results shown in Figure 4 indicates that Al-Nb-B master alloys are the most effective. As their intrinsic potency is expected to be lower, due to the less effective growth restriction of Nb, their higher efficacy is due to the higher chemical stability of Nb-based substrates with respect to Ti-based substrates and Al borides.

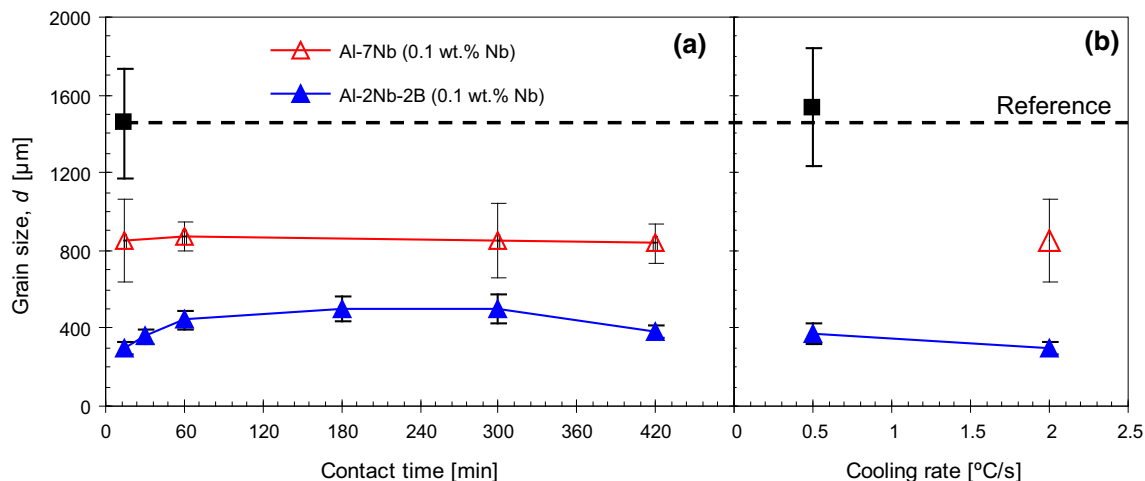


Fig. 4—Variation of the grain size (d) for the reference A354 alloy inoculated with Nb-based master alloys. (a) Effect of contact time and (b) effect of cooling rate.

IV. DISCUSSION

A. Effect of Heterogeneous Nucleation Substrates

Over the years, different theories have been proposed to understand the grain refinement of Al: carbide-boride particle theory,^[26] the peritectic theory,^[27] the hypernucleation theory,^[28] the duplex theory,^[29] and the solute theory.^[30] Semi-empirical models based on the constitutional undercooling were also lately proposed to relate the grain size to the growth restriction factor.^[31,32] The *free-growth model* proposed by Greer *et al.*^[31] states that grain initiation on a potent substrate is controlled by the barrier to growth of a nucleus, which depends on the dimension of the substrate:

$$\Delta T_{fg} = \frac{4\sigma}{\Delta S_v d_{sub}} \quad [1]$$

where ΔT_{fg} is the undercooling for free growth, σ is the liquid–solid interfacial energy, ΔS_v is the entropy of fusion per unit volume, and d_{sub} is the diameter of the substrate. Thus, the size of the substrate is critical for the formation of new grains where the largest particles become active nucleants at lower undercoolings.

Figure 5 shows representative results of the characterization of the master alloys used in this study. Full characterization of commercial Al-Ti-B master alloys has been previously reported.^[31] Blocky Al_3Ti and a fine dispersion of hexagonal platelets TiB_2 particles is generally found^[14] where for the latter particles below $0.2 \mu\text{m}$ and above $6.0 \mu\text{m}$ in diameter are barely present. Within this range, especially for diameters $> 1 \mu\text{m}$, the population distribution can be well fitted by an exponential function: $y = y_0 \exp(-d/d_0)$.^[31] The features (type, morphology, and size of the particles) of the Al-Ti-B master alloys were confirmed *via* SEM analysis (Figure 5(a)) and fully justify the fading of the grain

refining potency of the Ti-based heterogeneous substrates shown in Figure 2.

Al-B master alloys have also previously been extensively characterized.^[14,33] AlB_2 particles are generally predominant but the high-temperature AlB_{12} phase could also be present if the Al-B master alloys have been produced at temperatures lower than the peritectic reaction temperature.^[34] AlB_2 and AlB_{12} particles have hexagonal close packed and tetragonal crystal structures with $a = 3.006 \text{ \AA}$ and $c = 3.252 \text{ \AA}$ and $a = 10.161 \text{ \AA}$ and $c = 14.238 \text{ \AA}$ lattice parameters, respectively.^[35] The size and distribution of the particles are comparable to those of the TiB_2 particles found in Al-Ti-B master alloys and AlB_2 and AlB_{12} are present in the Al-5B master alloys (Figure 5(b)). As the A354 alloy used in this study has 0.12 pct Ti (see Table I) and Ti borides are more thermodynamically stable than Al borides, Al borides will progressively dissolve^[36] once the A354 alloy is inoculated with Al-5B (fading in Figure 3).

The Al-7Nb master alloy is characterized by a uniform dispersion of polygonal Al_3Nb particles (Figure 5(c)). The mean particle size of these peritectic particles is coarser in comparison to those found in the commercial master alloys (Figure 5(d)). Al_3Nb intermetallic particles form peritectically in liquid Al (and for 7 pct Nb they are stable up to approximately $1580 \text{ }^\circ\text{C}$ ^[24]) and are thus the heterogeneous substrates responsible for the grain refinement achieved. This study demonstrates and confirms that Al_3Nb particles are stable at temperature normally used in Al foundries and have the ability to refine the grain structure of Al-Si alloys (Figure 4).

Microstructural analysis confirms that stable heterogeneous substrates, with a particle size distribution from sub-micrometric ($0.5 \mu\text{m}$) to micrometers ($\sim 10 \mu\text{m}$), are present in the lab made Al-2Nb-2B master alloy and their dispersion and distribution is rather uniform. SEM

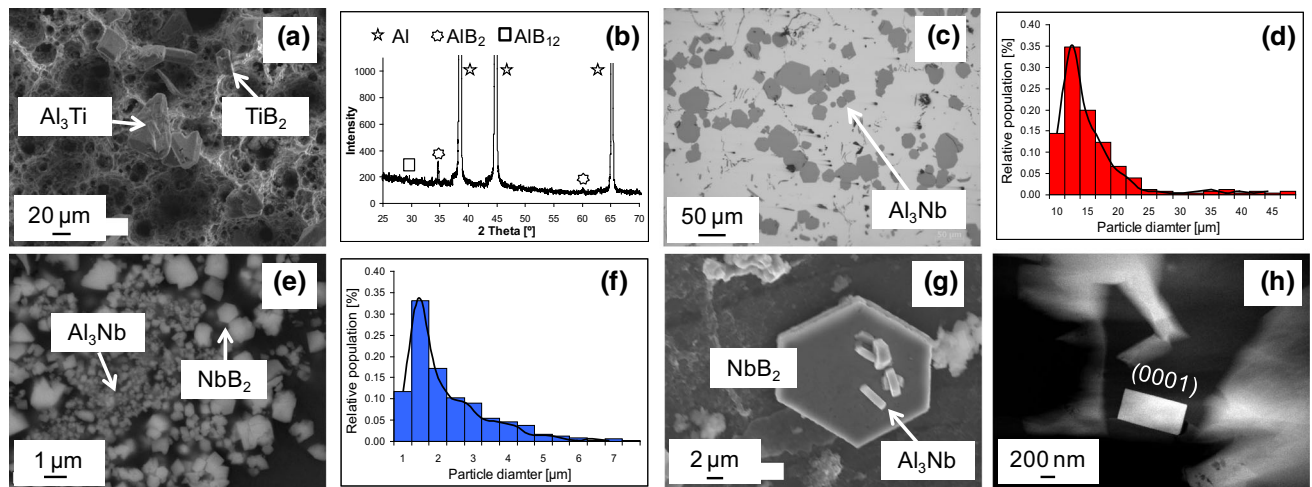


Fig. 5—Representative results of the characterization of the master alloys used. (a) SEM micrographs showing the particles present in the Al-Ti-B master alloys; (b) XRD pattern of the Al-5B master alloy; (c) optical micrograph showing the distribution of the particles present in the Al-7Nb master alloy; (d) size distribution of the Al_3Nb particles found in the Al-7Nb master alloy; (e) SEM micrograph showing the particles present in the Al-2Nb-2B master alloy; (f) size distribution of the particles present in the Al-2Nb-2B master alloy; (g) SEM micrograph showing the morphology of the particles of the Al-2Nb-2B master alloy; (h) HAADF-STEM micrograph of NbB_2 particle present in the Al-2Nb-2B master alloy showing the (0001) basal plane.

analysis indicates that two types of Nb-based compounds are present, NbB_2 and Al_3Nb as confirmed by EDS semi-quantitative analysis, and the compounds are actually agglomeration of various particles as outcome of the liquid engineering manufacturing method used to produce the Al-2Nb-2B master alloy.^[25] Although found in the concentrated Al-2Nb-2B master alloy, the particles disperse once added to the molten metal. SEM morphological analysis carried out in deep-etched Al-2Nb-2B master alloy samples and TEM investigation confirm the expected hexagonal (NbB_2) and tetragonal (Al_3Nb) crystal lattices as shown in Figure 5(g) where Al_3Nb particles nucleated onto the surface of a NbB_2 particles. High-angle annular dark field (HAADF) scanning transmission electron microscopy further confirmed the chemistry and morphology of the Nb-based heterogeneous substrates. Of particular interest is the (0001) basal plane of the NbB_2 compounds (see Figure 5(h)) which is the one with the lowest lattice mismatch and the most favorable orientation relationship to promote heterogeneous nucleation of α -Al grains as well as Al_3Nb crystals. The lattice constants for NbB_2 and for Al_3Nb are $a = 3.102 \text{ \AA}$ and $c = 3.285 \text{ \AA}$ and $a = 3.8485 \text{ \AA}$ and $c = 8.615 \text{ \AA}$, respectively.^[25]

The heterogeneous substrates added into the A354 alloy *via* the Ti-based, B-based, and Al-2Nb-2B master

alloys have comparable size and distribution. Assuming that the liquid–solid interfacial energy and the entropy of fusion do not significantly change, from Eq. [1] the ΔT_{fg} for the free growth of grains is similar for the different inoculants used. The comparison of the grain refinement achieved is done in Figure 6(a) where the best performance of each master alloy and addition rate, which in every fading experiment corresponds to the shortest inoculation time of 15 minutes, is presented. The Al_3Nb particles present in the Al-7Nb master alloy have bigger size which means that the nucleation of the primary α -Al grains commences at lower undercooling. As the grain refinement performance is dominated by the largest particles,^[31] the inoculation of the A354 alloy *via* an Al-Nb master alloy with Al_3Nb particles whose size is comparable to that of the other master alloys would require larger undercooling. On the basis of Spittle's works,^[37,38] a more straightforward comparison of the grain refining potency should be done considering a common element rather than the addition rate (Figure 6(a)) as the latter could lead to misjudgments.

The A354 alloy used in this study already contains ~ 0.12 pct Ti and all the master alloys, with the exception of the Al-7Nb, contain B; therefore, both elements could theoretically be used for a more sensible comparison. The variation of the grain size with the Ti and B

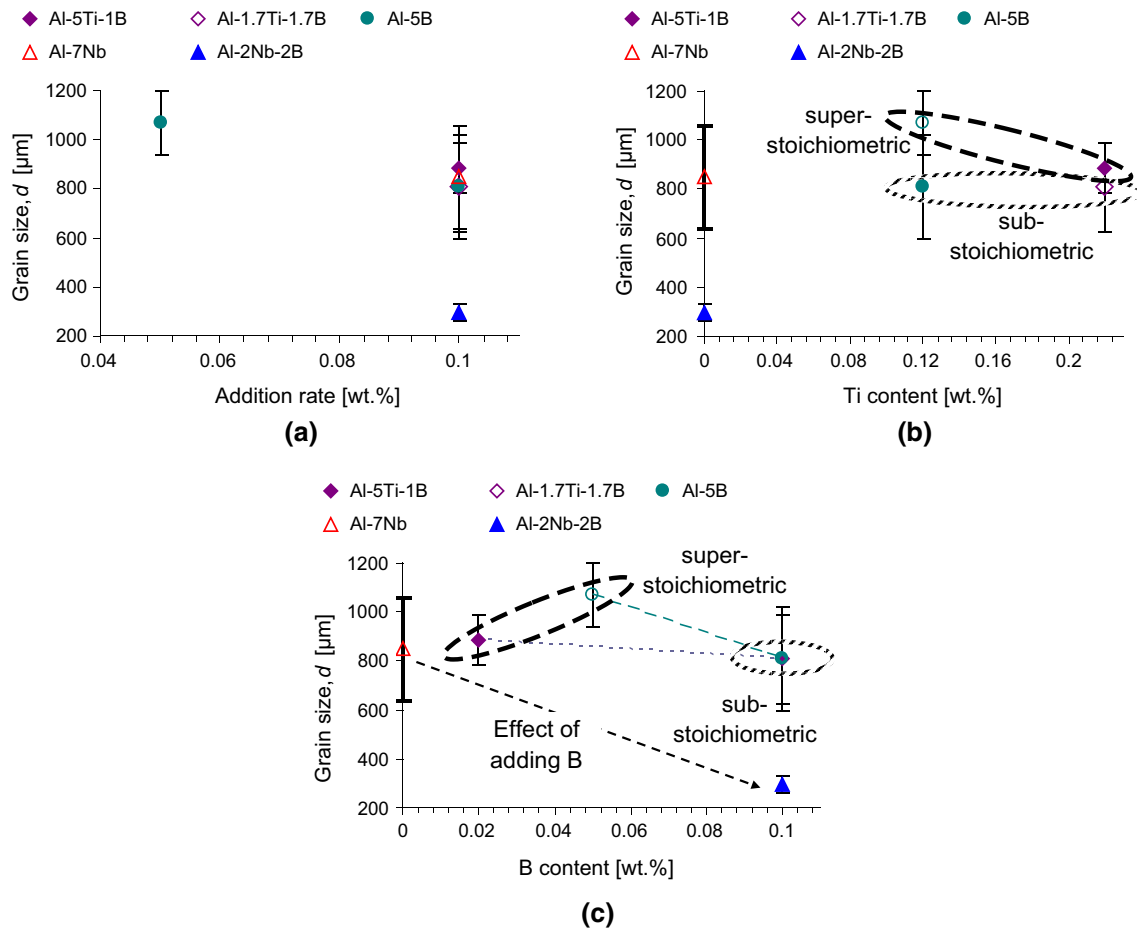


Fig. 6—Comparison of the inoculation efficacy of the different master alloys. (a) Variation of the grain size (d) with the addition rate; (b) variation of the grain size (d) with the Ti content; and (c) variation of the grain size (d) with the B content.

contents is plotted in Figures 6(b) and (c), respectively. The former permits to highlight the effect of the stoichiometry of the master alloys as the addition of 0.05 and 0.1 pct *via* the Al-5B master alloy results in Ti/B ratios of 2.4 (hyper-stoichiometric) and 1.2 (sub-stoichiometric), respectively. Consistent with the literature, sub-stoichiometric Ti-based master alloys, and by extension sub-stoichiometric B-based master alloy when Ti is present as impurity, have higher grain refining potency in Al-Si alloys than their respective hyper-stoichiometric counterparts for the same Ti content (see Table III). On the contrary, a higher amount of hyper-stoichiometric Ti-based master alloy, with the equivalent associated cost, would have to be used to obtain comparable grain sizes to those achieved *via* sub-stoichiometric master alloys. Regarding Figure 6(b), it is worth mentioning that the data relative to the Nb-based master alloys are plotted considering that the amount of Ti is zero as Al₃Nb and NbB₂ are supposed to be stable in the presence of Ti. We previously demonstrated that the Al-2Nb-2B master alloy is highly effective in refining the cast structure of Al-Si alloys regardless of the presence of Ti.^[19,20]

The data plotted in Figure 6(c) reinforce the finding that master alloys with higher amount of B (*i.e.*, sub-stoichiometric), or conversely lower amount of Ti, permit to obtain finer grain sizes. Nevertheless, focusing on hyper-stoichiometric master alloys, a higher amount of Ti is more beneficial, at least initially. At short inoculation times the diffusion-controlled chemical reaction between the Ti-based particles and Si is still

limited and thus, comparatively, there are more particles in the Al-5Ti-1B master alloy that can act as heterogeneous nucleation substrates than in the case of Al-5B + 0.12 pctTi. However, for longer contact time, their potency is similar (Figures 2 vs 3) due to the progression of the Ti-Si interaction. From Figure 6(c), although the Al-7Nb and the Al-2Nb-2B master alloys have quite different amount of Nb, it can still be pointed that the presence of B, and thus of NbB₂ particles, is needed to significantly increase the potency of Nb-based master alloys.

B. Effect of Alloy Chemistry

Alloy chemistry is another decisive factor that significantly affects nucleation outcomes and thus the effectiveness of the inoculation procedure. The solute segregation in front of the solid-liquid interface contributes by restricting the growth of the grains and generate constitutional undercooling that promote further nucleation events. The contribution of the solute is normally taken into account using the growth restriction factor ($Q = m \cdot (k - 1) \cdot C_0$ where m is the gradient of the liquidus, k is the partition coefficient, and C_0 is the alloy composition), and it is predicted that as Q increases, the grain size first decreases sharply, and then levels off when $Q \geq 15$.^[31] To estimate the influence of Q , purposely selected alloy chemistry (Table II) and addition rates (Table III) were used to obtain similar Q values. Five groups were obtained: $Q = 58, 75, 85, 95,$ and 110 K (see Table IV) where each Q value was calculated by summing the individual contribution of

Table III. Details of the Master Alloys and Addition Rates Used as well as Total Amount of Ti, B, and Nb Present in the Molten A354 Alloy

Alloy	Master Alloy	Addition Rate	Ti (Wt Pct)	B (Wt Pct)	Nb (Wt Pct)
A354	—	—	0.12	—	—
	Al-5Ti-1B	0.1 pct Ti	0.22	0.02	—
	Al-1.7Ti-1.7B	0.05 pct Ti	0.17	0.05	—
		0.1 pct Ti	0.22	0.10	—
	Al-5B	0.05 pct B	0.12	0.05	—
		0.1 pct B	0.12	0.10	—
	Al-7Nb	0.1 pct Nb	0.12	—	0.10
	Al-2Nb-2B	0.05 pct Nb	0.12	0.05	0.05
		0.1 pct Nb	0.12	0.10	0.10

Table IV. Grouping of the Alloys Studied (Table II) on the Basis of Growth Restriction Factor (Q)

Addition	Addition Rate (Pct)	Group 1 ($Q \sim 58$ K)	Group 2 ($Q \sim 75$ K)	Group 3 ($Q \sim 85$ K)	Group 4 ($Q \sim 95$ K)	Group 5 ($Q \sim 110$ K)
—	—	A1	A2, A3	—	A4	—
Al-5Ti-1B	0.1	—	—	A1	—	—
Al-1.7Ti-1.7B	0.05	—	—	A2	—	A4
	0.1	—	—	—	A2	A4
Al-5B	0.05	A1	A2, A3	—	A4	—
	0.1	A1	A2, A3	—	A4	—
Al-2Nb-2B	0.05	A1	A2, A3	—	A4	—
	0.1	A1	A2, A3	—	A4	—

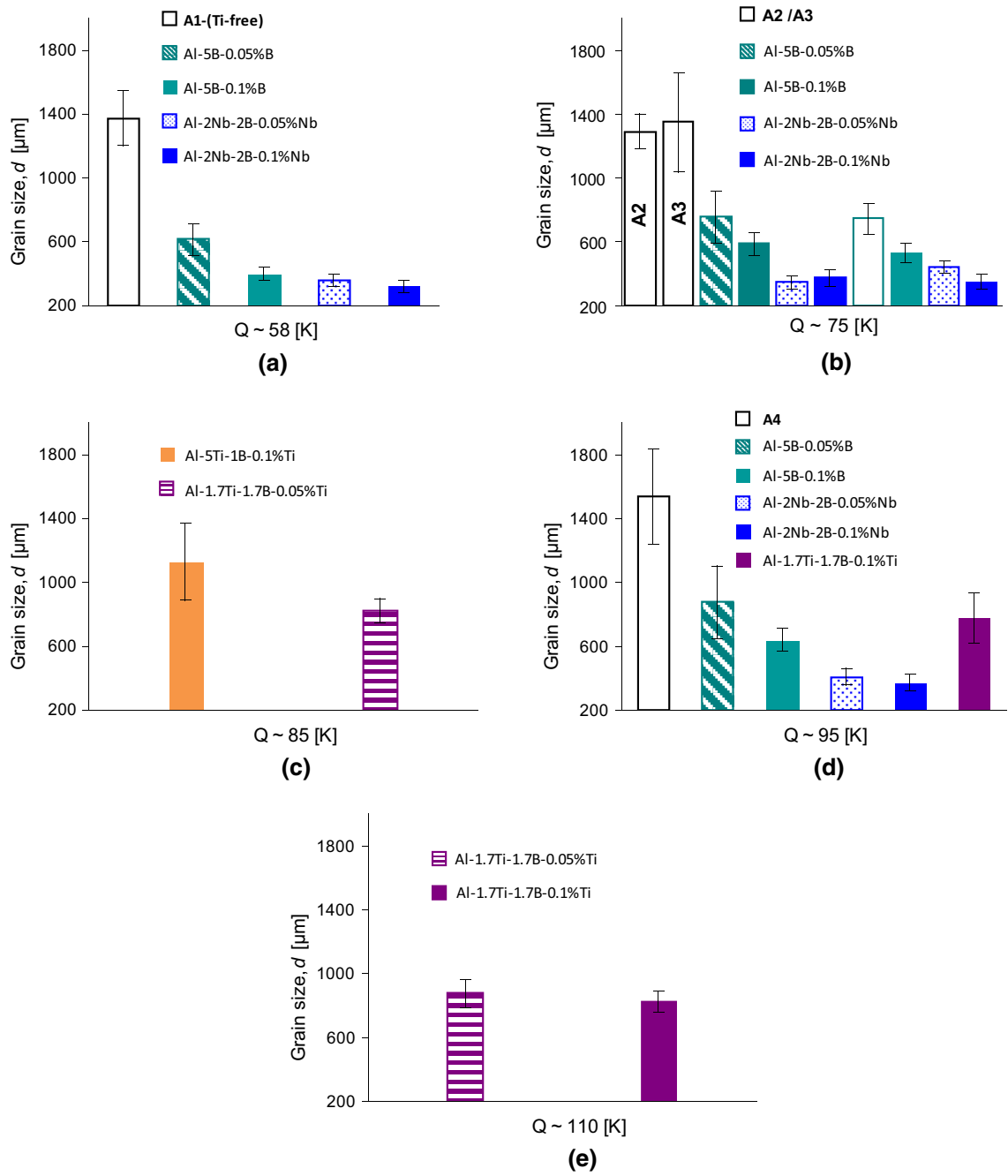


Fig. 7—Variation of the grain size (d) with Q (growth restriction factor): (a) $Q \sim 58$ K; (b) $Q \sim 75$ K; (c) $Q \sim 85$ K; (d) $Q \sim 95$ K; and (e) $Q \sim 110$ K.

solute (i) and for that the values of m and k provided in Reference 39 were used:

$$Q = \sum m_i \cdot (k_i - 1) \cdot C_{o,i} \quad [2]$$

The concept of growth restriction was further developed by Easton and St. John^[40] into a model to investigate and compare the grain refinement efficiency which relates the grain size (d) to the inverse of Q using a simple relationship:

$$d = a + b/Q \quad [3]$$

where a is a constant connected to the maximum number of particles that can be successfully activated as nucleants and b is a constant related to the potency of the nucleant particles present into or intentionally added to the molten metal.

Figure 7 illustrates the difference in grain size for the Q values groups listed in Table IV and it can be noticed that, contrary to previous reports,^[39,41] for Al-Si alloys the grain size does not decrease with Q as “A4” ($Q \sim 95$) as coarser grains than “A1” ($Q \sim 58$). Moreover, there are significant variations within alloys with the

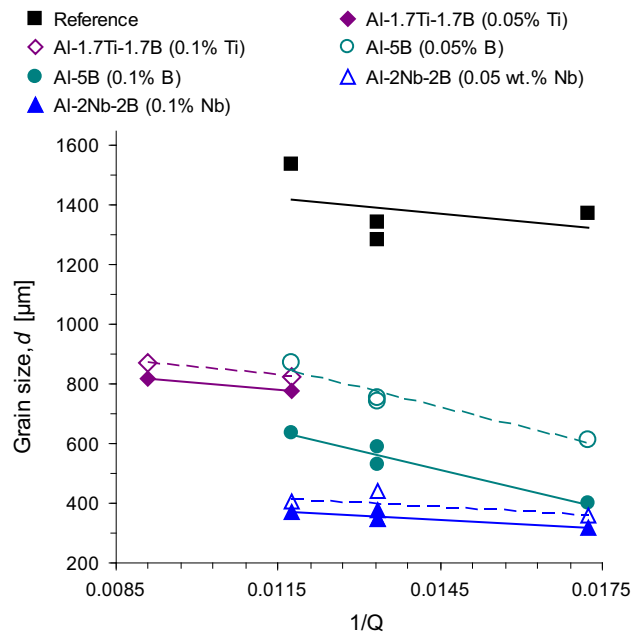


Fig. 8—Variation of the grain size (d) with $1/Q$.

Table V. Values of the a and b Parameters of Eq. [3] for Al-Si Alloys Without and With Chemical Inoculation

Material	Addition Rate	a	b	b (Average)
Reference	—	1625	− 17237	—
Al-1.7Ti-1.7B	0.05 pct Ti	1046	− 19036	− 17595
	0.1 pct Ti	966	− 16154	
Al-5B	0.05 pct B	1361	− 44173	− 43527
	0.1 pct NB	1135	− 42881	
Al-2Nb-2B	0.05 pct Nb	522	− 9555	− 9689
	0.1 pct Nb	489	− 9822	

same Q value and, generally, a higher addition of master alloy results in finer grain sizes at short inoculation time. At each Q value, the finest grain sizes are achieved using Nb-based heterogeneous substrates *via* the Al-2Nb-B master alloy, followed by the B-based particles (Figures 7(b) and (d)). As per Figure 7(c), it is confirmed that Al-1.7Ti-1.7B (sub-stoichiometric) performs better than Al-5Ti-1B (hyper-stoichiometric). A remark should be made about Figure 7(a): B- and Nb-based master alloys show much more similar potency as, conversely to the other alloys, the “Al” alloy is Ti-free (Table II). From this analysis, it is evident that the positive effect of adding different solutes *via* the master alloys is not exclusively due to the restriction imposed to the growing grains.

To further elucidate the effect of the alloy chemistry, the variation of the mean grain size with the inverse of Q is shown in Figure 8. It can be noticed that a linear trend is found for the alloys prior (squares) and after chemical inoculation. As per Eq. [3], the model developed by Easton and St. John^[40] predicts that the higher the Q value the finer the grain size. This is readily seen and achieved in wrought aluminum alloys, as data obtained

from these types of alloys were used to develop the model. However, the data of Figure 8 show grain coarsening with the Q value for both unrefined and refined alloys as the Q value is determined by the alloy chemistry as per Eq. [2]. The data presented in Figure 8 also indicate that the model can still be applied but, in the case of cast Al-Si alloys, the slope b is negative as the grain size increases for higher Q values. The difference in intercept a values suggests that different numbers of heterogeneous particles were active and triggered nucleation events. Generally lower a values are obtained with higher addition rates due to the presence of more particles initially acting as active nucleants.

The values of the intercept a and slope b obtained *via* linear regression analysis of the data plotted in Figure 8 are reported in Table V confirming that different a values are obtained for different addition rates as the higher the addition rate the higher the number of potential active heterogeneous nucleation substrates.

It can also be noticed that slightly different values are reported in terms of the slope b as a function of the addition rate. This is mainly due to the highly heterogeneous non-equiaxed dendritic grains which lead to a high variance of the average values. Furthermore, the different average values of the slope b highlight that the master alloys, and therefore the inoculants present (*i.e.*, TiB_2/Al_3Ti in Al-Ti-B, Al borides in Al-B, and NbB_2/Al_3Nb in Al-Nb-B as per Figure 5), have different potency. This is easily understandable for the Al-B master alloys, as Al borides have significantly different features (*i.e.*, structure and lattice parameters) with respect to TiB_2 and NbB_2 , and the grain size becomes coarser much faster with the increase of the Q value. Nevertheless, as per Figure 5 TiB_2/Al_3Ti in Al-Ti-B and NbB_2/Al_3Nb in Al-Nb-B are isomorphous and have similar lattice parameters^[25] and thus they could potentially have the same potency. The difference found is then most likely related to the poisoning of the inoculants once in contact with the molten Al-Si alloy.

V. CONCLUSIONS

From this study about the effect of boride particles and inoculation variables on the grain refinement of Al-Si alloys, the following conclusions can be drawn:

1. Ti-, Al-, and Nb-based boride and niobium aluminide particles can act as nucleation sites for α -Al but they have significantly different potency which, in most cases, is affected by the alloy chemistry and casting conditions. When the comparison of the potency of the master alloys is done considering a common element rather than the addition rate, sub-stoichiometric Al-Ti-B master alloys, generally, perform better than their hyper-stoichiometric counterparts.
2. Ti-based master alloys, containing TiB_2 and Al_3Ti , refine to some extent the cast structure of Al-Si alloys. However, the potency of the master alloys is rapidly lost due to poisoning as the contact time increases.

- The addition of B-based master alloys grain refine Al-Si alloys. When the Al-Si alloy contains Ti as impurity, B-based and Ti-based master alloys show comparable potency and similarly cannot completely prevent the formation of columnar grains. For B-based master alloys, higher addition rates lead to finer grain sizes but there is also a greater influence from the casting conditions.
- Nb-based master alloys consistently refine Al-Si alloy where the finest grain sizes are obtained when both Nb and B are present. The Al-7Nb master alloy has comparable efficacy to those of Ti- and B-based master alloys but the efficacy is not affected by the presence of the alloying elements such as Si or the contact time.
- Alloy chemistry affects the level of refinement and a linear relationship between the grain size (d) and the inverse of the growth restriction factor ($1/Q$) is found but the slope b is negative as unrefined and refined cast Al-Si alloys are characterized by grain coarsening as Q increases.

ACKNOWLEDGMENTS

The authors are thankful for the financial support from the Technology Strategy Board (TSB) through the TSB/101177 Project and to the Engineering and Physical Sciences Research Council (EPSRC) through the EP/J013749/1 and EP/K031422/1 Projects.

DATA AVAILABILITY

All metadata pertaining to this work can be accessed via the following link: <https://doi.org/10.17633/rd.brunel.7332854>.

OPEN ACCESS

This article is distributed under the terms of the Creative Commons Attribution 4.0 International License (<http://creativecommons.org/licenses/by/4.0/>), which permits unrestricted use, distribution, and reproduction in any medium, provided you give appropriate credit to the original author(s) and the source, provide a link to the Creative Commons license, and indicate if changes were made.

REFERENCES

- S.K. Shaha, F. Czerwinski, W. Kasprzak, J. Friedman, and D.L. Chen: *J. Alloys Compd.*, 2014, vol. 615, pp. 1019–31.
- M.A. Easton, M. Qian, A. Prasad, and D.H. St. John: *Curr. Opin. Solid State Mater. Sci.*, 2016, vol. 20, pp. 13–24.

- R. Schmid-Fetzer and A. Kozlov: *Acta Mater.*, 2011, vol. 59, pp. 6133–44.
- M. Johnsson: *Zeitschrift für Metallkunde*, 1984, vol. 85, pp. 781–85.
- G.S.V. Kumar, B.S. Murty, and M. Chakraborty: *J. Alloys Compd.*, 2009, vol. 472, pp. 112–20.
- D. Qiu, J.A. Taylor, M.X. Zhang, and P.M. Kelly: *Acta Mater.*, 2007, vol. 55, pp. 1447–56.
- V.E. Bazhenov and M.A. Magura: *Mater. Sci. Technol.*, 2018, vol. 34, pp. 1287–94.
- A. L. Greer: *J. Chem. Phys.*, 2016, vol. 145, art. no. 211704.
- T. Wang, H. Fu, Z. Chen, J. Xu, J. Zhu, F. Cao, and T. Li: *J. Alloys Compd.*, 2012, vol. 511, pp. 45–49.
- Y. Birol: *Mater. Sci. Technol.*, 2012, vol. 28, pp. 481–86.
- L. Yu, X. Liu, Z. Wang, and X. Bian: *J. Mater. Sci.*, 2005, vol. 40, pp. 3865–67.
- H. Zhao, H. Bai, J. Wang, and S. Guan: *Mater. Charact.*, 2009, vol. 60, pp. 377–83.
- P. Li, S. Liu, L. Zhang, and X. Liu: *Mater. Des.*, 2013, vol. 47, pp. 522–28.
- Y. Birol: *J. Alloys Compd.*, 2012, vol. 513, pp. 150–53.
- Y. Birol: *Mater. Sci. Technol.*, 2012, vol. 28, pp. 385–89.
- A. N. Kolmogorov and S. Curtarolo: *Phys. Rev. B*, 2006, vol. 74, art. no. 224507.
- X. Wang: *J. Alloys Compd.*, 2017, vol. 722, pp. 302–06.
- J. Li, G. Yang, F.S. Hage, Z. Chen, T. Wang, Q.M. Ramasse, and P. Schumacher: *Mater. Charact.*, 2017, vol. 128, pp. 7–13.
- L. Bolzoni, M. Nowak, and N. Hari Babu: *Mater. Sci. Eng. A*, 2015, vol. 628, pp. 230–37.
- L. Bolzoni and N. Hari Babu: *J. Mater. Process. Technol.*, 2015, vol. 222, pp. 219–23.
- L. Bolzoni and N. Hari Babu: *Mater. Lett.*, 2017, vol. 201, pp. 9–12.
- L. Bolzoni, M. Nowak, and N. Hari Babu: *J. Alloys Compd.*, 2015, vol. 623, pp. 79–82.
- Z. Chen, T. Wang, L. Gao, H. Fu, and T. Li: *Mater. Sci. Eng. A*, 2012, vol. 553, pp. 32–36.
- V.T. Witusiewicz, A.A. Bondar, U. Hecht, and T.Y. Velikanova: *J. Alloys Compd.*, 2009, vol. 472, pp. 133–61.
- L. Bolzoni, M. Xia, and N. Hari Babu: *Sci. Rep.*, 2016, vol. 6, art. no. 39554.
- A. Cibula: *J. Inst. Met.*, 1951, vol. 80, pp. 1–16.
- F.A. Crossley and L.F. Mondolfo: *J. Met. (Trans. AIME)*, 1951, vol. 191, pp. 1143–48.
- Solidification Processing*, ed., G.P. Jones, and J. Beech, and H. Jones, eds., *Solidification Processing*, University of Sheffield, Sheffield, 1998, pp. 496–97.
- P.S. Mohanty and J.E. Gruzleski: *Acta Metall. Mater.*, 1995, vol. 43, pp. 2001–12.
- I. Maxwell and A. Hellawell: *Acta Metall.*, 1975, vol. 23, pp. 229–37.
- A.L. Greer, A.M. Bunn, A. Tronche, P.V. Evans, and D.J. Bristow: *Acta Mater.*, 2000, vol. 48, pp. 2823–35.
- M.A. Easton and D.H. St. John: *Acta Mater.*, 2001, vol. 49, pp. 1867–78.
- Z. Chen, H. Kang, G. Fan, J. Li, Y. Lu, J. Jie, Y. Zhang, T. Li, X. Jian, and T. Wang: *Acta Mater.*, 2016, vol. 120, pp. 168–78.
- S. Nafisi and R. Ghomashchi: *Mater. Sci. Eng. A*, 2007, vols. 452–453, pp. 445–53.
- X. Wang: *J. Alloys Compd.*, 2005, vol. 403, pp. 283–87.
- V.T. Witusiewicz, A.A. Bondar, U. Hecht, J. Zollinger, L.V. Artyukh, and T.Y. Velikanova: *J. Alloys Compd.*, 2009, vol. 474, pp. 86–104.
- J.A. Spittle: *Foundry Trade J.*, 2008, vol. 10, pp. 335–40.
- J.A. Spittle: *Foundry Trade J.*, 2008, vol. 10, pp. 308–14.
- M. Easton and D.H. St. John: *Metall. Mater. Trans. A*, 1999, vol. 30, pp. 1613–23.
- M. Easton and D. St. John: *Metall. Trans. A*, 2005, vol. 36A, pp. 1911–20.
- P.S. Mohanty and J.E. Gruzleski: *Acta Mater.*, 1996, vol. 44, pp. 3749–60.